RHEOLOGY AND FLOW DYNAMICS OF LUNAR LAVA FLOWS. Edward Davis[1], Lionel Wilson[1,2], Yuan Chen[2,3], and James Head[2], [1]Lancaster Environment Centre, Lancaster University, U.K. [2]Department of Earth, Environmental and Planetary Sciences, Brown University, U.S.A. [3]Key Laboratory of Lunar and Deep Space Exploration, National Astronomical Observatories, Chinese Academy of Sciences, China.

Introduction: The large volumes of lunar mare lava flows imply their formation from the eruption of isolated dikes transferring magma rapidly from the deep mantle to the surface [1] at near-liquidus temperatures. The inevitable result is a high-volume eruption rate. Coupled with the low viscosities of mare lavas [2,3,4], this implies that the lava leaving the vent area will be turbulent [1]. Turbulence causes the entire flow to radiate heat rapidly [5]. On the timescale (days [6]) of the emplacement of high eruption-rate mare lava flows, heat loss to ground that might initiate erosion to create a sinuous rille channel [5] can be neglected [7]. The decrease in temperature, T, causes an increase in liquid viscosity and progressive crystallization induces non-Newtonian rheology. We model this with a Bingham rheology [8], characterized by a yield strength Y and plastic viscosity η. These are both functions of the crystal fraction X(T) and are obtained from experimental data [9, 10, 11]:

$$Y = 0, X < 0.021 \quad (1)$$

$$Y = 2.95\times10^{-4} \{[(X/0.021) - 1] /[1 - (X/0.45)]\}^{3.509}, X > 0.021 \quad (2)$$

$$\eta = f_v (1477.15 / T)^{10.0207} \quad (3)$$

$$f_v = [1 - (X / 0.6)]^{-2.5}, X < 0.317 \quad (4)$$

$$f_v = \exp\{[2.5+(X/(0.6 - X))^{0.48}] (X/0.6)\}, X > 0.317 \quad (5)$$

The influence of Y and η on the flow regime is monitored via the dimensionless Reynolds number, Re = (4 ρ U D)/η, and Hedström number, He = (16 D^2 Y ρ) / η^2 [8], where U and D are the flow's mean speed and depth, and ρ is the lava density. Decreasing temperature increases X, which increases He, which increases the critical Reynolds number, Re_{crit}, that allows turbulence. Simultaneously, increasing *X* causes a decrease in the actual Re from its initially high value. If Re falls below Re_{crit}, turbulence ceases, the flow becomes laminar, and thermal boundary layers start to form at all flow margins with waves of cooling penetrating slowly into the flow. However, the isothermal core of the flow is insulated by these boundary layers and preserves the extremely non-Newtonian rheology that it had at the moment of turbulent-to-laminar transition. This is in stark contrast to a flow that is laminar throughout its motion. If an all-laminar flow is erupted at a high temperature, it will have a near-Newtonian rheology in its core with only the growing boundary layers exhibiting non-Newtonian rheology. The key issues are therefore (a) how far from the vent do initially turbulent mare lava flows remain turbulent, (b) what effects does the turbulent-to-laminar transition have on their morphology, and (c) can they become turbulent again after first becoming laminar? We explore these issues using morphologic observations on the distal part of a well-preserved flow in Mare Imbrium (Fig. 1).

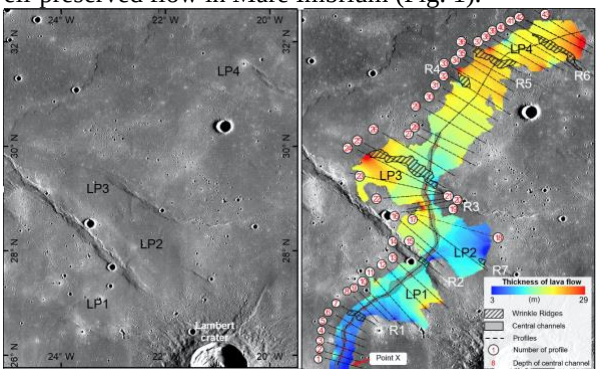

Figure 1. The distal part of the studied Mare Imbrium lava flow located between Mons La Hire and Lambert crater [12].

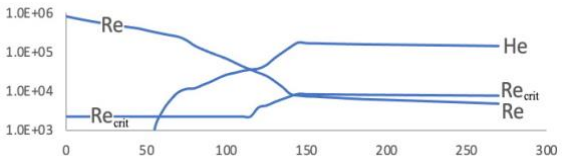

Figure 2. Variation of the Reynolds number, Re, Hedström number, He, and critical Reynolds number, Re_{crit}, with distance in km from the vent.

Analysis: Figure 2 shows how Re, He and Re_{crit} change with distance from the vent for a modeled initially turbulent mare lava flow. Turbulence ends when the decreasing Re becomes just less than Re_{crit}. The flow core is then protected thermally by the as-yet thin boundary layers, and there is no reason, other than changes in the slope of the ground over which the flow is moving, why the values of Re, He and Re_{crit} should change until those boundary layers appreciably invade the isothermal core. Figure 2 shows an increasing gap between the Re and Re_{crit} curves only because the slope in this model changes monotonically from 0.002 to 0.0004 radians between the vent and flow terminus to simulate an eruption from a mare basin margin into the shallower basin interior. However, there is no reason why the slope should decrease steadily. The present mare surface shows significant changes in slope due to movement along faults associated with wrinkle ridges that were active after the flow was

emplaced (Fig. 3), but there are other changes not directly linked to faults. In places the flow widens (see Fig. 1a) before crossing the location of a wrinkle ridge implying that there was ponding of the flow in a depression linked to pre-eruption ridge development. Collectively these observations imply significant topographic irregularities along the path of the flow at the time of its formation.

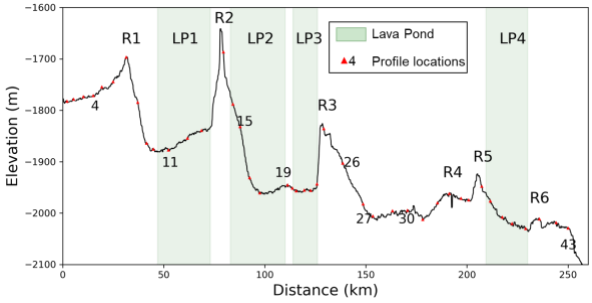

Figure 3. Along-flow topography showing links between wrinkle ridges (R) and lava ponds (LP).

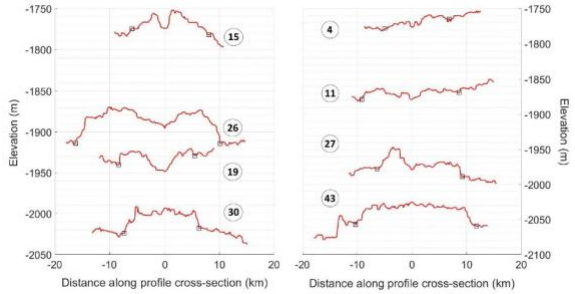

Figure 4. Examples of topographic profiles across the flow. Small squares indicate likely flow margins

To explore the influence of substrate slope changes we measured 43 topographic profiles (Fig. 4) across the flow (locations in Fig. 1b) and used formulae from [13] to find the yield strength Y from both the widths, W_l, and the maximum thicknesses, (approximated by the maximum thickness of the flow, D), of levees wherever they could be identified:

$$Y = \rho g D \sin \alpha \quad (6)$$

$$Y = (\rho g D^2)/(2 W_l) \quad (7)$$

where g is the acceleration due to gravity and α is the down-flow slope. To estimate α, we fitted a low-order polynomial to the profile in Fig. 3 to attempt to minimize the effects of the elevation changes due to post-eruption fault movements. The yield strength was used to find the crystal content X and this was used to find the plastic viscosity η. The standard formulae for turbulent and laminar flow of Bingham plastics [8] were then used to find U, D, Re, He and Re_{crit} to evaluate whether the flow was laminar or turbulent.

Results: Y increased along the part of the flow studied, from quartiles of ~80 to ~128 Pa using eq. (6) and ~65 to ~138 using eq. (2). However, using eq. (6), Y first decreased with distance along the flow before increasing to its final value, whereas using eq. (7), which does not involve the slope, Y increased steadily as expected (with "noise" due to the difficulty of locating the edges of the flow). Using parameters derived from the values of Y from eq. (7), Figure 5 summarizes the main result of the analysis: the flow appears to have made transitions back and forth between turbulent and laminar flow at various points along its path as it interacted with changes of slope and topographic obstacles, an activity predicted by [14].

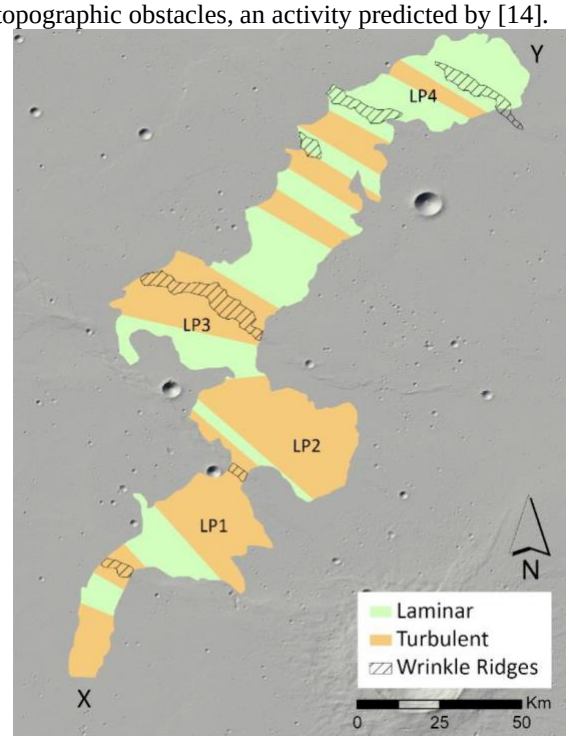

Figure 5. Zone locations of turbulent or laminar flow.

References: [1] Wilson, L., Head, J.W., 2017. *Icarus 283*, 146. [2] Murase T., McBirney A., 1970. *Science 167(3924)*, 1491. [3] Cukierman M., et al., 1973. *GCA 3*, 2685. [4] Williams, D.A. et al., 2000. *JGR 105(20)*, 189. [5] Hulme, G., 1973. *Modern Geology 4*, 107. [6] Wilson, L., Head, J.W., 2018. *GRL 45(12)*, 5852. [7] Hulme, G., 1982. *Surv. Geophys. 5*, 245. [8] Skelland, A.H.P., 1967. *Non-Newtonian Flow and Heat Transfer*. Wiley. [9] Jeffrey, D.J., Acrivos, A., 1976. *AICE Journal 22(3)*, 417. [10] Pinkerton, H., Stevenson, R.J., 1992. *JVGR 53*, 47. [11] Ishibashi, H., Sato, H., 2010. *J. Min. Pet. Sci. 105*, 334. [12] Chen, Y., et al., 2021, LPSC 52, #1818. [13] Hulme, G., 1974. *Geophys. J. Roy. Astron. Soc. 39*, 361. [14] Glaze, L.S., et al., 2014. *JGR: Solid Earth, 119*, 1837.